

ST-MFNET MINI: KNOWLEDGE DISTILLATION-DRIVEN FRAME INTERPOLATION

Crispian Morris, Duolikun Danier, Fan Zhang, Nantheera Anantrasirichai and David R. Bull

Bristol Vision Institute, University of Bristol, One Cathedral Square, Bristol, BS1 5DD, UK.
 {crispian.morris, duolikun.danier, fan.zhang, n.anantrasirichai, dave.bull}@bristol.ac.uk

ABSTRACT

Currently, one of the major challenges in deep learning-based video frame interpolation (VFI) is the large model sizes and high computational complexity associated with many high performance VFI approaches. In this paper, we present a distillation-based two-stage workflow for obtaining compressed VFI models which perform competitively to the state of the arts, at a greatly reduced model size and complexity. Specifically, an optimisation-based network pruning method is first applied to a recently proposed frame interpolation model, ST-MFNet, which outperforms many other VFI methods but suffers from large model size. The resulting new network architecture achieves a 91% reduction in parameters and 35% increase in speed. Secondly, the performance of the new network is further enhanced through a teacher-student knowledge distillation training process using a Laplacian distillation loss. The final low complexity model, ST-MFNet Mini, achieves a comparable performance to most existing high-complex VFI methods, only outperformed by the original ST-MFNet. Our source code is available at <https://github.com/crispianm/ST-MFNet-Mini>.

Index Terms—Video frame interpolation, model compression, knowledge distillation

I. INTRODUCTION

Video frame interpolation (VFI) is a widely used technique for increasing the temporal resolution of videos. Recently, deep learning algorithms have enabled a significant boost in the performance of VFI methods [1], and these have been employed extensively in various applications, such as for video compression, slow motion content rendering and view synthesis [2].

Existing works on VFI generally rely on deep neural networks (DNNs). While flow-based VFI methods [3–5] estimate the optical flow to perform frame warping, kernel-based methods [6–8] predict per-pixel interpolation kernels to synthesise the target frame. Recent advances in both classes of methods include the use of coarse-to-fine architectures [9, 10], multi-stage/branch pipelines [2, 11–13], 3D convolution [14, 15], and self-attention mechanisms [16, 17]. Although the latest developments have continuously improved the state-of-the-art performance on commonly used benchmarks, it is observed from many methods that there is a tendency to adopt more and more complex network

designs, resulting in large model sizes and higher computational complexity. For example, the recently proposed model ST-MFNet [2] contains 21 million parameters, takes approximately 82MB to store in FP32 (32 bit floating point precision) and requires much longer runtime than much simpler VFI approaches (e.g., $45\times$ compared to AdaCoF [7]). Such a large model is inefficient in both training and inference (thus having high carbon footprint [18]), posing high memory requirements on hardware and preventing deployment in real-world scenarios.

In order to tackle the problem of large model sizes and high complexity, techniques such as model pruning [19] and knowledge distillation [20] are commonly utilised. One of the few efforts made to apply these to VFI is [21], where the AdaCoF [7] model was pruned using a sparsity-inducing optimisation objective [22] to obtain a small network with evidently decreased performance. Newly designed model components were then integrated into this small model to enhance its performance. It is noted that although a large compression ratio was achieved by pruning the model, the additional components that contributed to the performance gain of the pruned model doubled its size.

In this work, we leverage knowledge distillation to achieve model compression for VFI. This allows a compact model to obtain favourable performance against the state of the arts, without including any additional modules. Specifically, we design a two-stage pipeline (illustrated in Figure 1) to compress ST-MFNet - a recent model with state-of-the-art VFI performance. In the first stage, we follow [21] to adopt a sparsity-induced model pruning technique, OBProx-SG [22], to obtain a new, compact ST-MFNet with 91% reduction in parameters. In the second stage, we train it with a novel knowledge distillation loss so it ‘learns’ additional information from the ‘teacher’ model (a pre-trained original ST-MFNet). The resulting low complexity VFI approach, ST-MFNet Mini, is able to outperform its ‘teacher’ in certain cases, with significantly reduced model size and complexity. To the best of our knowledge, this is the first attempt in VFI that employs knowledge distillation for the purpose of model compression. The proposed framework can potentially be applied to other VFI methods to reduce their model complexity.

THE WORK WAS FUNDED BY THE UNIVERSITY OF BRISTOL, THE UKRI MYWORLD STRENGTH IN PLACES PROGRAMME (SIPF00006/1), AND CHINA SCHOLARSHIP COUNCIL.

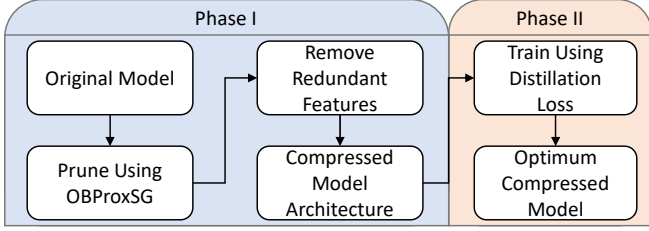


Fig. 1: The proposed VFI compression workflow. Phase I: model size and complexity reduction. Phase II: interpolation quality enhancement.

II. PROPOSED METHOD

In this work, we configure the model the same as in [2], that given four consecutive frames $\{I_0, I_1, I_2, I_3\}$, the VFI method outputs I_t where $t = 1.5$ to achieve $\times 2$ interpolation. In this section, we first describe ST-MFNet’s architecture and the process of pruning it (Phase I in Figure 1), followed by the knowledge distillation process used to train the compact ST-MFNet, which we dub ‘ST-MFNet Mini’ (Phase II).

II-A. Pruning ST-MFNet

Given four input frames, the original ST-MFNet first processes them in two branches: MIFNet and BLFNet. While the former uses a U-Net style model to predict per-pixel deformable interpolation kernels, the latter employs a pre-trained optical flow estimator to obtain one-to-one pixel correspondence. These estimated kernels and optical flows are then used to synthesise the target middle frame. The results are passed to a GridNet [23], from which we obtain an intermediate interpolation result, \tilde{I}_t . This is combined with all four input frames and fed to a 3D CNN to estimate the textural residuals, denoted as R . Final output is obtained by $\tilde{I}_t + R$. Readers are referred to the original paper for more details.

Sparsity inducing optimisation. In order to obtain a condensed version of ST-MFNet, we start with the original pre-trained model, which is publicly available, and fine-tune the original model with the following loss function,

$$\mathcal{L}_{\text{Charb}}(I_{\text{pred}}, I_{\text{gt}}) = \sqrt{(I_{\text{pred}} - I_{\text{gt}})^2 + \epsilon^2}, \quad (1)$$

$$\mathcal{L}_{\text{prune}} = \mathcal{L}_{\text{Charb}}(I_{\text{pred}}, I_{\text{gt}}) + \lambda \|\theta\|_1 \quad (2)$$

where I_{gt} and I_{pred} are the ground-truth target frame and the prediction of ST-MFNet respectively, and $\epsilon = 0.001$. The parameters of ST-MFNet are denoted as θ , and $\|\theta\|_1$ refers to the l_1 norm regularisation term, which induces sparsity in the network [22]. Such sparsity information can be used as a guide to remove redundant layers in the network. We adopt the OBProx-SG [22] solver to perform the optimisation, which has been shown to be efficient for sparsity-based model pruning [21].

Similarly to [21], we define each layer, l , in the model as $l = [C_{\text{out}}, C_{\text{in}}, q_0, q_1, q_2]$, with total number of parameters

$p_l = C_{\text{out}} \cdot C_{\text{in}} \cdot q_0 \cdot q_1 \cdot q_2$. As training takes place, we calculate the density (d) for each layer l using

$$d_l = \frac{\# \text{ of nonzero weights in } l}{p_l}, \quad (3)$$

and use these values to compute the average density in the model as an indicator for the training progress. Following [21], we set $\lambda = 10^{-4}$ and optimise the network for 20 epochs using our combined training set (Sec. III-A), achieving a density of approximately 0.24.

Network compression. The sparsity-inducing optimisation above allows us to see, through the final layer densities, the individual layers in the network which contribute less to the overall model performance, and thus can be removed or shrunk. Therefore, starting with the final layer, we use its density as its compression ratio (r_n), forming a new layer in the form

$$l'_n = [C_{\text{out}}, r_n \cdot C_{\text{in}}, q_0, q_1, q_2],$$

and causing

$$l'_{n-1} = [r_{n-1} \cdot C_{\text{out}}, C_{\text{in}}, q_0, q_1, q_2].$$

We iterate through the model’s n layers this way, as in [24], ensuring that each layer’s outputs match the previously compressed layer’s inputs.

For ST-MFNet, we found that the flow estimator component of the model (BLFNet) has near-zero compression ratios, so it is removed entirely instead of shrunk. Ultimately, this process prunes the model from 21.03M parameters to 1.82M, a 91% reduction in number of parameters. The architecture of the pruned network (ST-MFNet Mini) is shown in Figure 2

II-B. Knowledge Distillation

To verify the effectiveness of the distillation loss, a ‘baseline’ model is created by training the pruned model obtained from the previous stage on the ground-truth data using Laplacian loss (the same training conditions as ST-MFNet). We note that after 20 epochs this baseline shows decreased average performance compared to the original model (shown in Table I in Sec. III).

In order to enhance the performance of the pruned model, the previous work [21] added new components to the model, which increased the model size. In contrast, we devise a knowledge distillation loss for VFI, where the pruned ‘student’ network learns additional information from the pre-trained original ST-MFNet, the ‘teacher’ network, without any increase in size.

Specifically, the loss function used to train the student network consists of two components. Firstly, the loss between the ground truth and the student model’s prediction ($\mathcal{L}_{\text{stud}}$), and secondly, the loss between the student and the teacher’s predictions ($\mathcal{L}_{\text{dist}}$). The total loss for the model is therefore

$$\mathcal{L}_{\text{total}} = \alpha \mathcal{L}_{\text{stud}}(I_{\text{out}}, I_{\text{gt}}) + \mathcal{L}_{\text{dist}}(I_{\text{pred}}, I_{\text{out}}), \quad (4)$$

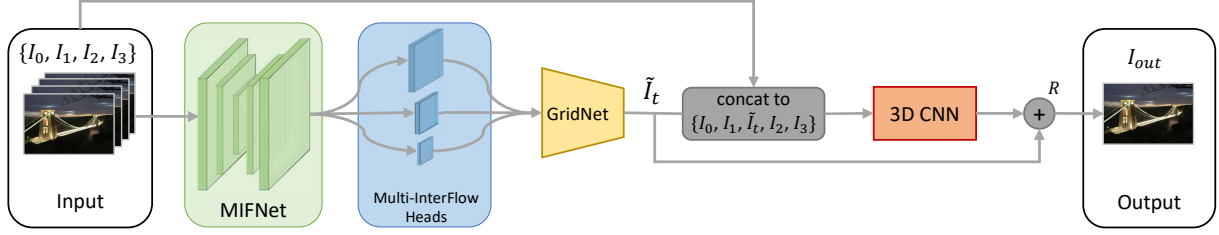


Fig. 2: The resulting model architecture of ST-MFNet Mini.

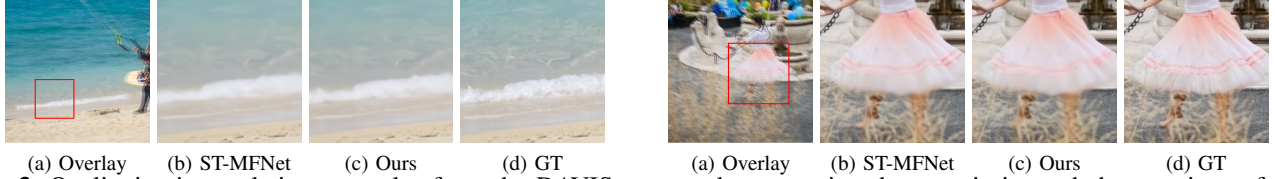


Fig. 3: Qualitative interpolation examples from the DAVIS test set demonstrating the superiority and shortcomings of our approach. The first column (a) shows the overlaid adjacent frames, while the final column (d) contains the ground truth frame.

where I_{gt} represents the ground truth frame, I_{out} represents the student model’s output, and I_{pred} represents the original model’s prediction. Here, α is a hyper-parameter controlling the penalty from the ground-truth frames.

The student network is trained from scratch using the loss function (Eqn. 4), enabling the pruned network to make use of the additional knowledge learned by the teacher network in prior training.

III. RESULTS AND DISCUSSION

III-A. Experimental Setup

Implementation details. The student model is trained for 20 epochs on the same training set as the pre-trained teacher model, i.e. approximately 92K frame quintuplets, from the Vimeo90K septuplet [25] and BVI-DVC [26] datasets. We use Laplacian pyramid loss as both \mathcal{L}_{stud} and \mathcal{L}_{dist} , and AdaMax [27] with $\beta_1 = 0.9, \beta_2 = 0.999$. The hyper-parameter α in Eqn. 4 is set to 0.1, based on empirical results.

Evaluation. The model is evaluated on multiple commonly used test datasets, including UCF101, DAVIS, and SNU-Film. Two commonly used metrics, PSNR and SSIM [28], are adopted to evaluate the frame interpolation performance.

III-B. Ablation Study

The baseline and Laplacian distilled models are compared in Table I. It is clear to see that the distillation process improves model performance greatly. To investigate potential further improvements, particularly in the perceptual realm, several GAN-based loss functions are tested as the distillation loss function. Specifically, we test the following adversarial functions: GAN [29], ST-GAN [30], and FIGAN [7]. These are trained for 10 epochs on the same training set, with the same hyperparameters as before. However, they fail to

improve on the effectiveness of the Laplacian distillation, so they are not trained further.

III-C. Qualitative Evaluation

Visual comparisons. Examples of frames interpolated using our model and ST-MFNet are shown in Figure 3. In some conditions, the model’s results are observably closer to the ground truth than ST-MFNet, as evidenced in the first case, while for footage with large movement, such as the second case, the model’s performance suffers slightly.

III-D. Quantitative Evaluation

The comprehensive quantitative evaluation results are summarised in Table I. It is noted that the Laplacian-trained compressed model (ST-MFNet Mini) outperforms its teacher on two databases: SNU-FILM Easy and Extreme, while its performance on databases with large motions are not as good as the state of the arts. This may be explained by the fact that the BLFNet component of the model was removed, which was shown to improve the model’s ability to handle large motion [2].

Figure 4 plots the mean PSNR values of all the tested VFI approaches against their model parameters. It can be observed that STMFNet Mini achieved an excellent trade off between performance, with the lowest model size but second best overall performance. The model with the second least model parameters, CDFI, is nearly three times as large.

However, while the compressed model outperforms for its size, it does not meet the same expectations for its runtime. Despite being 35% faster than the original ST-MFNet, the model is still much slower than other, large models. This is likely due to the upscaling component of ST-MFNet (3D CNN), which requires lengthy computation time. It is the focus of our future work.

Table I: Quantitative comparison results (PSNR/SSIM) for ST-MFNet Mini and 13 tested methods. In some cases, scores found using pre-trained models are provided, underlined, when they outperform their re-trained counterparts. For each column, the best result is bold in **red** and the second best is italicised in *blue*. The average runtime (RT) for interpolating a 480p DAVIS frame as well as the number of model parameters (#P) for each method are also reported.

	UCF101	DAVIS	SNU-FILM				RT (sec)	#P (M)
			Easy	Medium	Hard	Extreme		
SuperSloMo [3]	32.547/0.968	26.523/0.866	36.255/0.984	33.802/0.973	29.519/0.930	24.770/0.855	0.107	39.61
SepConv [6]	32.524/0.968	26.441/0.853	39.894/0.990	35.264/0.976	29.620/0.926	24.653/0.851	<i>0.062</i>	21.68
DAIN [11]	<u>32.524/0.968</u>	27.086/0.873	39.280/0.989	34.993/0.976	29.752/0.929	24.819/0.850	0.896	24.03
BMBC [31]	<u>32.729/0.969</u>	26.835/0.869	39.809/0.990	35.437/0.978	29.942/0.933	24.715/0.856	1.425	11.01
AdaCoF [7]	<u>32.610/0.968</u>	26.445/0.854	39.912/0.990	35.269/0.977	29.723/0.928	24.656/0.851	0.051	21.84
CDFI [21]	<u>32.653/0.968</u>	26.471/0.857	39.881/0.990	35.224/0.977	29.660/0.929	24.645/0.854	0.321	<i>4.98</i>
CAIN [8]	<u>32.537/0.968</u>	26.477/0.857	<u>39.890/0.990</u>	35.630/0.978	29.998/0.931	25.060/0.857	0.071	42.78
SoftSplat [5]	32.835/0.969	<u>27.582/0.881</u>	40.165/0.991	36.017/0.979	30.604/0.937	25.436/0.864	0.206	12.46
EDSC [32]	<u>32.677/0.969</u>	26.689/0.860	39.792/0.990	35.283/0.977	29.815/0.929	24.872/0.854	0.067	8.95
XVFI [33]	32.224/0.966	26.565/0.863	38.849/0.989	34.497/0.975	29.381/0.929	24.677/0.855	0.108	5.61
QVI [4]	32.668/0.967	27.483/ <i>0.883</i>	36.648/0.985	34.637/0.978	30.614/0.947	25.426/0.866	0.257	29.23
FLAVR [14]	<u>33.389/0.971</u>	27.450/0.873	40.135/0.990	35.988/0.979	30.541/0.937	25.188/0.860	0.695	42.06
ST-MFNet [2]	<i>33.384/0.970</i>	28.287/0.895	40.775/ 0.992	37.111/0.985	31.698/0.951	<i>25.810/0.874</i>	0.901	21.03
ST-MFNet Mini (Baseline)	33.013/0.968	26.013/0.848	<i>40.826/0.991</i>	35.858/0.980	30.724/0.946	25.726/ <i>0.891</i>	0.588	1.82
ST-MFNet Mini (KD Loss)	33.070/0.969	26.335/0.855	40.982/0.992	<i>36.127/0.982</i>	<i>30.914/0.950</i>	25.877/0.894	0.588	1.82

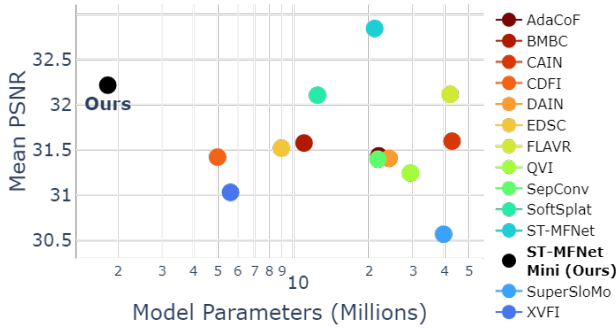


Fig. 4: Mean PSNR scores from the models presented in Table I. On average, our method outperforms all models except its teacher, at a greatly reduced size.

IV. CONCLUSION

In this paper, a workflow for frame interpolation model compression was presented which utilises model pruning to determine a reduced model architecture and knowledge distillation to improve its performance. This method was applied to an advanced VFI approach, ST-MFNet, and the resulting low complexity model (ST-MFNet Mini) only requires 9% of the original model’s parameters to achieve competitive interpolation performance, compared to the state-of-the-art approaches. Future work should focus on generalising this workflow to other VFI approaches, employing more effective knowledge distillation implementations (e.g., feature based) during training in the second stage and significantly reducing the model runtime.

REFERENCES

- [1] J. Dong, K. Ota, and M. Dong, “Video Frame Interpolation: A Comprehensive Survey,” *ACM Transactions on Multimedia Computing, Communications and Applications*, 2022.
- [2] D. Danier, F. Zhang, and D. Bull, “ST-MFNet: A spatio-temporal multi-flow network for frame interpolation,” in *Proceedings of the IEEE/CVF Conference on Computer Vision and Pattern Recognition*, 2022, pp. 3521–3531.
- [3] H. Jiang, D. Sun, V. Jampani, M.-H. Yang, E. Learned-Miller, and J. Kautz, “Super sloMo: High quality estimation of multiple intermediate frames for video interpolation,” in *Proceedings of the IEEE Conference on Computer Vision and Pattern Recognition*, 2018, pp. 9000–9008.
- [4] X. Xu, L. Siyao, W. Sun, Q. Yin, and M.-H. Yang, “Quadratic video interpolation,” in *NeurIPS*, 2019.
- [5] S. Niklaus and F. Liu, “Softmax splatting for video frame interpolation,” in *Proceedings of the IEEE/CVF Conference on Computer Vision and Pattern Recognition*, 2020, pp. 5437–5446.
- [6] S. Niklaus, L. Mai, and F. Liu, “Video frame interpolation via adaptive separable convolution,” in *Proceedings of the IEEE International Conference on Computer Vision*, 2017, pp. 261–270.
- [7] H. Lee, T. Kim, T.-y. Chung, D. Pak, Y. Ban, and S. Lee, “Adacof: Adaptive collaboration of flows for video frame interpolation,” in *Proceedings of the IEEE/CVF Conference on Computer Vision and Pattern Recognition*, 2020, pp. 5316–5325.
- [8] M. Choi, H. Kim, B. Han, N. Xu, and K. M. Lee, “Channel attention is all you need for video frame interpolation,” in *Proceedings of the AAAI Conference on Artificial Intelligence*, vol. 34, 2020, pp. 10 663–10 671.
- [9] F. Reda, J. Kontkanen, E. Tabellion, D. Sun, C. Pantofaru, and B. Curless, “FILM: Frame interpolation for large motion,” in *Computer Vision—ECCV 2022: 17th European Conference, Tel Aviv, Israel, October 23–27, 2022, Proceedings, Part VII*. Springer, 2022, pp. 250–266.
- [10] L. Kong, B. Jiang, D. Luo, W. Chu, X. Huang, Y. Tai, C. Wang, and J. Yang, “Ifnet: Intermediate feature refine network for efficient frame interpolation,” in *Proceedings of the IEEE/CVF Conference on Computer Vision and Pattern Recognition*, 2022, pp. 1969–1978.
- [11] W. Bao, W.-S. Lai, C. Ma, X. Zhang, Z. Gao, and M.-H. Yang, “Depth-aware video frame interpolation,” in *Proceedings of the IEEE/CVF Conference on Computer Vision and Pattern Recognition*, 2019, pp. 3703–3712.
- [12] W. Bao, W.-S. Lai, X. Zhang, Z. Gao, and M.-H. Yang, “Memc-net: Motion estimation and motion compensation

- driven neural network for video interpolation and enhancement,” *IEEE transactions on pattern analysis and machine intelligence*, vol. 43, no. 3, pp. 933–948, 2019.
- [13] S. Gui, C. Wang, Q. Chen, and D. Tao, “Featureflow: Robust video interpolation via structure-to-texture generation,” in *Proceedings of the IEEE/CVF Conference on Computer Vision and Pattern Recognition*, 2020, pp. 14 004–14 013.
 - [14] T. Kalluri, D. Pathak, M. Chandraker, and D. Tran, “Flavr: Flow-agnostic video representations for fast frame interpolation,” *arXiv preprint arXiv:2012.08512*, 2020.
 - [15] D. Danier, F. Zhang, and D. Bull, “Enhancing deformable convolution based video frame interpolation with coarse-to-fine 3d cnn,” in *2022 IEEE International Conference on Image Processing (ICIP)*. IEEE, 2022, pp. 1396–1400.
 - [16] L. Lu, R. Wu, H. Lin, J. Lu, and J. Jia, “Video frame interpolation with transformer,” in *Proceedings of the IEEE/CVF Conference on Computer Vision and Pattern Recognition*, 2022, pp. 3532–3542.
 - [17] Z. Shi, X. Xu, X. Liu, J. Chen, and M.-H. Yang, “Video frame interpolation transformer,” in *Proceedings of the IEEE/CVF Conference on Computer Vision and Pattern Recognition*, 2022, pp. 17 482–17 491.
 - [18] A. Lacoste, A. Luccioni, V. Schmidt, and T. Dandres, “Quantifying the carbon emissions of machine learning,” *arXiv preprint arXiv:1910.09700*, 2019.
 - [19] R. Reed, “Pruning algorithms-a survey,” *IEEE transactions on Neural Networks*, vol. 4, no. 5, pp. 740–747, 1993.
 - [20] G. Hinton, O. Vinyals, and J. Dean, “Distilling the knowledge in a neural network,” *arXiv preprint arXiv:1503.02531*, 2015.
 - [21] T. Ding, L. Liang, Z. Zhu, and I. Zharkov, “CDFI: Compression-driven network design for frame interpolation,” in *Proceedings of the IEEE/CVF Conference on Computer Vision and Pattern Recognition*, 2021, pp. 8001–8011.
 - [22] T. Chen, T. Ding, B. Ji, G. Wang, Y. Shi, J. Tian, S. Yi, X. Tu, and Z. Zhu, “Orthant based proximal stochastic gradient method for l_1 -regularized optimization,” in *Machine Learning and Knowledge Discovery in Databases: European*
 - [23] *Conference, ECML PKDD 2020, Ghent, Belgium, September 14–18, 2020, Proceedings, Part III*. Springer, 2021, pp. 57–73.
 - [24] D. Fourure, R. Emonet, E. Fromont, D. Muselet, A. Tremeau, and C. Wolf, “Residual conv-deconv grid network for semantic segmentation,” *arXiv preprint arXiv:1707.07958*, 2017.
 - [25] T. Chen, B. Ji, Y. Shi, T. Ding, B. Fang, S. Yi, and X. Tu, “Neural network compression via sparse optimization,” *arXiv preprint arXiv:2011.04868*, 2020.
 - [26] T. Xue, B. Chen, J. Wu, D. Wei, and W. T. Freeman, “Video enhancement with task-oriented flow,” *International Journal of Computer Vision*, vol. 127, no. 8, pp. 1106–1125, 2019.
 - [27] D. Ma, F. Zhang, and D. Bull, “BVI-DVC: A training database for deep video compression,” *IEEE Transactions on Multimedia*, pp. 1–1, 2021.
 - [28] D. P. Kingma and J. Ba, “Adam: A method for stochastic optimization,” *arXiv preprint arXiv:1412.6980*, 2014.
 - [29] Z. Wang, A. C. Bovik, H. R. Sheikh, and E. P. Simoncelli, “Image quality assessment: from error visibility to structural similarity,” *IEEE transactions on image processing*, vol. 13, no. 4, pp. 600–612, 2004.
 - [30] I. Goodfellow, J. Pouget-Abadie, M. Mirza, B. Xu, D. Warde-Farley, S. Ozair, A. Courville, and Y. Bengio, “Generative adversarial networks,” *Communications of the ACM*, vol. 63, no. 11, pp. 139–144, 2020.
 - [31] works,” in *2016 IEEE 13th International Conference on Signal Processing (ICSP)*. IEEE, 2016, pp. 1135–1139.
 - [32] J. Park, K. Ko, C. Lee, and C.-S. Kim, “BMBC: Bilateral motion estimation with bilateral cost volume for video interpolation,” in *Computer Vision–ECCV 2020: 16th European Conference, Glasgow, UK, August 23–28, 2020, Proceedings, Part XIV 16*. Springer, 2020, pp. 109–125.
 - [33] X. Cheng and Z. Chen, “Multiple video frame interpolation via enhanced deformable separable convolution,” *IEEE Transactions on Pattern Analysis and Machine Intelligence*, 2021.
 - [34] H. Sim, J. Oh, and M. Kim, “XVFI: extreme video frame interpolation,” in *Proceedings of the IEEE International Conference on Computer Vision (ICCV)*, 2021.